Multiobjective Optimization of the Continuous Casting Process for Poly (methyl methacrylate) Using Adapted Genetic Algorithm

FANGBIN ZHOU, SANTOSH K. GUPTA,* AJAY K. RAY

Department of Chemical and Environmental Engineering, National University of Singapore, 10 Kent Ridge Crescent, Singapore 119260, Singapore

Received 19 October 1999; accepted 1 March 2000

ABSTRACT: The nondominated sorting genetic algorithm (NSGA) has been used to optimize the operation of the continuous casting of a film of poly (methyl methacrylate). This process involves two reactors, namely, an isothermal plug flow tubular reactor (PFTR) followed by a nonisothermal film reactor. Two objective functions have been used in this study: the cross-section average value of the monomer conversion, $\bar{x}_{mf}$, of the product is maximized, and the length, z_f, of the film reactor is minimized. Simultaneously, the cross-section average value of the number-average molecular weight of the product is forced to have a certain prescribed (desired) value. It is also ensured that the temperature at any location in the film being produced lies below a certain value, to avoid degradation reactions. Seven decision variables are used in this study: the temperature of the isothermal PFTR, the flow rate of the initiator in the feed to the PFTR (for a specified feed flow rate of the monomer), the film thickness, the monomer conversion at the output of the PFTR, and three coefficients describing the wall temperature to be used in the film reactor. Sets of nondominating (equally good) optimal solutions (Pareto sets) have been obtained due to the conflicting requirements for the several conditions studied. It is interesting to observe that under optimal conditions, the exothermicity of the reactions drives them to completion near the center of the film, while heat conduction and higher wall temperature help to achieve this in the outer regions. © 2000 John Wiley & Sons, Inc. J Appl Polym Sci 78: 1439–1458, 2000

Key words: poly (methyl methacrylate); multiobjective optimization; genetic algorithm; pareto set; film casting

INTRODUCTION

It is well known that poly methyl methacrylate (PMMA) is an important commodity plastic having several applications. Though the polymerization of methyl methacrylate (MMA) has been carried out in industry for a long time, several interesting problems on the modeling, optimization, and control of the reactors used for its polymerization still fascinate scientists and engineers. In this study, we report our efforts to model and optimize the film-casting process used in the manufacture of PMMA.

In industry, methyl methacrylate is frequently polymerized in bulk. In these operations, the autoacceleration (Trommsdorff or gel) effect plays an important role, and is associated with a sud-

Correspondence to: A. K. Ray.
S. K. Gupta is on leave from the Indian Institute of Technology, Kanpur, 208016, India.
* *Present address:* Department of Chemical Engineering, University of Wisconsin, Madison, WI 53706.

Journal of Applied Polymer Science, Vol. 78, 1439–1458 (2000)

den increase of the molecular weight of the polymer, as well as of the rate of reaction. A considerable amount of research[1–14] has been reported on the modeling of this diffusion-limited phenomenon. This has been reviewed by Gao and Penlidis[15] and Mankar et al.[16] The recent models[9,10,12] are quite robust, and general and can be used for the optimization of polymerizations under a variety of operating conditions. In this study, we use the model of Seth and Gupta[12] to simulate the nonisothermal production of a thin film of PMMA[6,17] and then optimize the process using multiple objective functions and constraints, using an adaptation[18] of genetic algorithm (GA).[19–21]

In contrast to work on the modeling of polymerization systems and reactors (including industrial units), which has attained a reasonable state of maturity in the open literature, work on the optimization of polymerization reactors has barely started.[22,23] In the early years, the less robust Pontryagin principle[24–26] was used. Unfortunately, this traditional optimization technique requires an excellent initial guess of the optimal solutions, and the results and the rate of convergence of the solution are very sensitive to these guesses. For complex systems, for example, the polymerization of methyl methacrylate, the "window" within which the initial guess must lie, is quite narrow,[27] and one must almost know the optimal solution one is trying to obtain. One method for going around this problem is to solve easier problems first[28,29] to get a good initial guess. This technique is quite slow, and is, therefore, not suited for on-line applications, which are of considerable current interest. In recent years, an extremely robust technique, genetic algorithm[19–21] (GA), and its adaptations[18,30] for more useful but complex multiobjective optimization problems, have become popular. These do not need any initial guesses, and converge to the global optimum[19–21] even when there are several local optima present. This algorithm is superior to traditional optimization algorithms in many aspects. It is better than calculus-based methods (both direct and indirect methods) that generally seek out the local optimum, and which may miss the global optimum. Most of the older techniques require values of the derivatives of the objective functions, and in most real-life problems, the existence of derivatives is questionable and often, the functions are discontinuous, multimodal, and noisy. In such cases, calculus-based methods fail. GA is superior to these techniques, because it is conceptually different from these traditional algorithms in several respects. It uses a population of several points simultaneously, and it works as well with probabilistic (instead of deterministic) operators. In addition, GA uses information on the objective function and not its derivatives, nor does it require any other auxiliary knowledge.[19–21]

In the last several years, some research has been reported in the open literature on the optimization of polymerization reactors using multiple objective functions and constraints, and its use in on-line optimizing control. In such cases, instead of obtaining a unique optimal solution, a set of equally good (nondominating) optimal solutions is usually obtained. These are referred to as Pareto sets. Rigorously, a Pareto set is defined,[31] for example, for a problem involving two objective functions, I_1 and I_2, as a set of points such that, when we move from any one point to another on this set, one objective function improves while the other worsens.[31] A decision maker can choose any one of these nondominant optimal solutions based on additional information that is often based on a "gut feeling" (and is nonquantifiable). Our group has reported some studies[32,33] on the use of one adaptation[18,30] of GA for well-mixed batch reactors for PMMA manufacture.

In earlier years, multiobjective optimization problems were usually solved using a single scalar objective function, which was a weighted average of the several objectives ("scalarization" of the vector objective function). This process allows a simpler algorithm to be used, but unfortunately, the solution obtained depends largely on the values assigned to the weighting factors used, which is done quite arbitrarily. An even more important disadvantage of the scalarization of the several objectives is that the algorithm may miss some optimal solutions, which can never be found, regardless of the weighting factors chosen. Several methods are available to solve multiobjective optimization problems, for example, the ϵ-constraint method, goal attainment method, and the nondominated sorting genetic algorithm (NSGA). In this study we use NSGA to obtain the Pareto set. This technique offers several advantages; for example (a) the efficiency of the method is relatively insensitive to the shape of the Pareto optimal front, (b) problems with uncertainties, stochasticities, and with discrete search spaces can be handled efficiently, (c) the "spread" of the Pareto

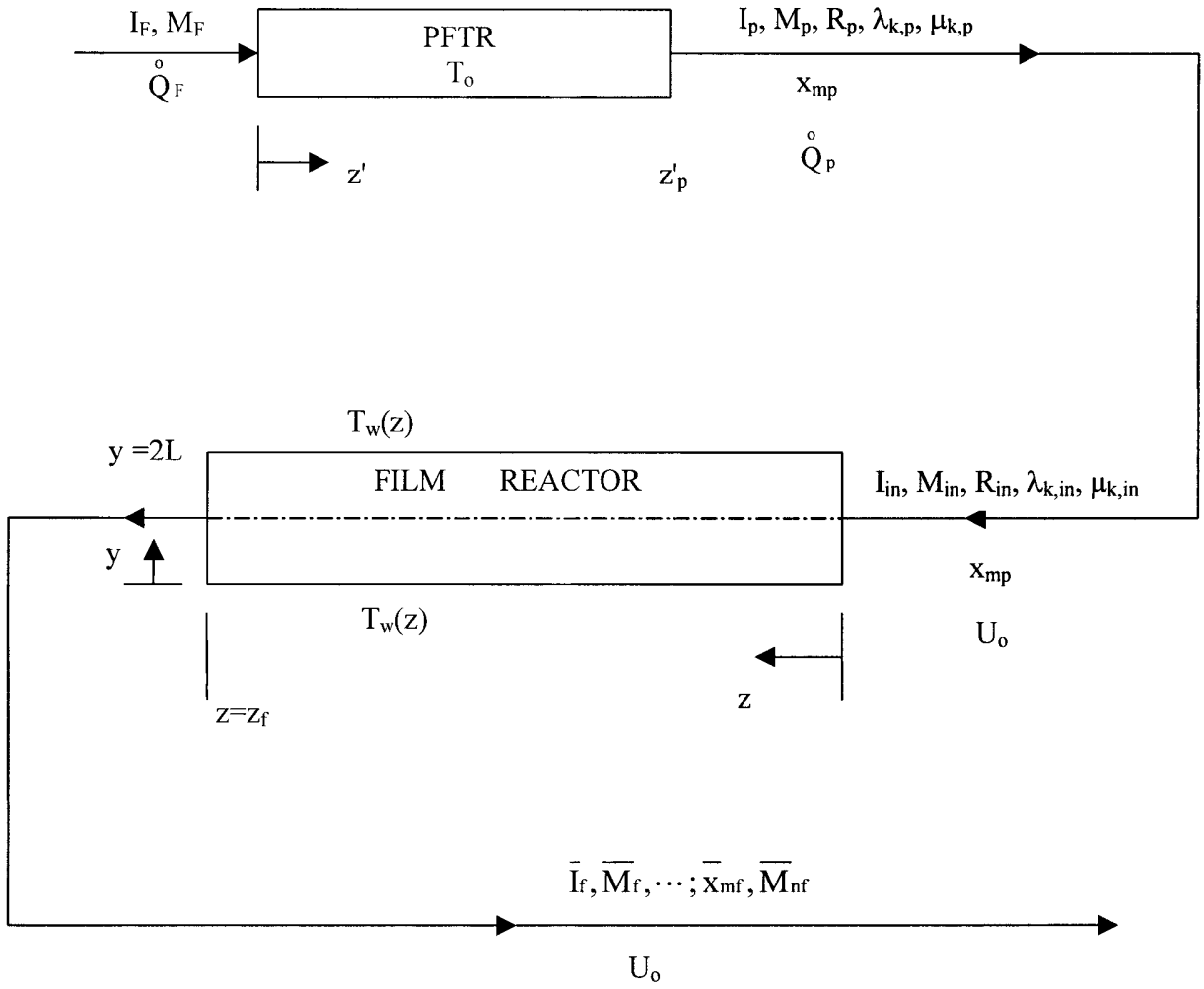

Figure 1 Flow diagram of the continuous casting process for PMMA films. $k = 0, 1, 2$. I_{in}, M_{in}, etc., $= I_p/(2LW)$, $M_p/(2LW)$, etc. $U_o = \dot{Q}_p/(2LW)$.

set obtained is excellent (in contrast, the efficiency of other optimization methods decides the spread of the solutions obtained); and (d) it involves a single application to obtain the entire Pareto set (in contrast to other methods, e.g., the ϵ-constraint method, which needs to be applied several times over). Indeed, NSGA has been used to solve a variety of multiobjective optimization problems in chemical engineering in recent years, as for example, an industrial nylon-6 semibatch reactor,[30] a wiped-film polyester reactor,[34] a steam reformer,[35] membrane modules,[36] and cyclone separators.[37] These form the subject of a recent review.[38]

In the present study, we report work on the multiobjective optimization of a more complex industrial process for PMMA, namely, the continuous casting of thin films of this polymer.[6,17] In this process, a well-mixed isothermal batch reactor (BR), or an isothermal plug-flow tubular reactor (PFTR), is used to obtain a prepolymer. This product is fed to a film reactor (see Fig. 1) where a thin film of the polymerizing mass flows inside a furnace with temperature programming. In the two-reactor sequence studied here, one important objective function is to maximize the final (i.e., at the end, $z = z_f$, of the film reactor) section average (i.e., average taken over the thickness, $0 \leq y \leq 2L$, of the film) value of the monomer conversion. The second objective function is to minimize the length, z_f, of the film reactor. An important end-point constraint that must be satisfied simul-

taneously is to ensure that the section average (across the thickness of the film) molecular weight of the final polymer film produced has a desired value. In addition, a global constraint on the temperature (which must be below a safe value anywhere in the film) must be used to ensure that there is no degradation of the polymer. These ensure good color and physical properties. Seven decision or design variables are optimized in this study (see Fig. 1). These are: the temperature, T_o, of operation of the BR/PFTR, the flow rate, I_F, of the initiator in the feed to the BR/PFTR (for a specified flow rate, M_F, of the monomer in the feed), the monomer conversion, x_{mp}, from the BR/PFTR, half the film thickness, L, and three coefficients, b_1, b_2, and b_3, describing the temperature at the film surface ($T_w = T_o + b_1 z + b_2 z^2 + b_3 z^3$, $0 \le z \le z_f$) in the film reactor. Alternate formulations of the multiobjective optimization problem could be written and solved, but we develop and illustrate the use of the technique only with the above problem.

It is to be mentioned here that the approximate values of the monomer conversion (~60%), number-average molecular weight (~10^6 g/mol) and temperature (50°C) in the stream emerging from the BR/PFTR under the optimal conditions obtained later in this article, are such that the viscosity of the prepolymer would be of the order of[16] 2.5×10^4 Pa-s. Special anchor agitators would have to be used in real batch reactors, both to ensure homogeneity in the reaction mass, as well as to have isothermal conditions. For the same reasons, "internal" coils or grids for heat transfer would be required in real tubular reactors. The velocity profiles in such tubular reactors with internals would almost be uniform across the cross section, and our use of equations for an ideal PFTR would, thus, be justified. At the beginning of the film reactor, there would be a short length where the velocity profile will change into a uniform one (equivalent to an entrance region). We believe that the errors due to these approximations are small enough.

FORMULATION

The continuous casting process[6,17] shown in Figure 1 is first modeled. In this process, a mixture of monomer and initiator is pumped into the PFTR (at rates M_F and I_F mol/s, respectively), and the monomer is polymerized to a desired conversion, x_{mp}, in this reactor. The prepolymer produced in this reactor, which has some structural strength, is then fed to a double-belt system (or furnace), where it continues to polymerize. The temperature, T_w, of the belts (at $y = 0$ and $2L$) is a function of z. Finally, the product is collected at the end of the film reactor in the form of a roll.

Table I Kinetic Scheme for Bulk Addition Polymerization of MMA

Initiation	$I \xrightarrow{k_d} 2R$
	$R + M \xrightarrow{k_i} p_1$
Propagation	$P_n + M \xrightarrow{k_p} P_{n+1}$
Termination (disproportionation)	$P_n + P_m \xrightarrow{k_t} D_n + D_m$

The kinetic scheme for the bulk polymerization of MMA is given in Table I. This table incorporates the important[32] reactions only. The mass balance and moment equations for the PFTR and the film reactor are given in Tables II and III, respectively. In Table II, the balance equations for the PFTR are written in terms of the molar flow rates (mol/s), I, M, R, λ_k, and μ_k ($k = 0, 1, 2$). These are more convenient for flow systems in which the density changes with position. It is assumed that the volume of the reaction mass at any location can be approximated as the sum of the volumes of the pure (unreacted) monomer and the pure polymer (produced). The volumetric flow rate at any axial location in this reactor is $\mathring{Q}$.

In the equations in Table III for the film reactor, I, M, R, λ_k, and μ_k ($k = 0, 1, 2$) are the molar flow rates per unit transverse area (mol/m^2-s). In this reactor, the temperature, concentrations and moments are functions of both the transverse (y) and the axial (z) locations. The y-dependence of temperature (and so, of the concentrations and the moments) arises because of the presence of a thermal resistance in that direction. In writing these equations, it is assumed that the density of the reaction mixture is constant at the value corresponding to the feed to this reactor (the same as at the output of the PFTR). This implies that the reaction mixture is flowing at a constant axial velocity, U_o. It may be mentioned that if the density changes were, indeed, accounted for (with the axial velocity uniform across the y-direction, as would be physically expected in the two-belt driven film), the thickness of the film would

Table II Model Equations for MMA Polymerization in the PFTR

0. $t = \dfrac{A_t z'}{\mathring{Q}_F}$

1. $\dfrac{dI}{dt} = (-k_d I)\dfrac{\mathring{Q}_F}{\mathring{Q}}$

2. $\dfrac{dM}{dt} = \left(-k_p \dfrac{\lambda_0 M}{\mathring{Q}} - k_i \dfrac{RM}{\mathring{Q}}\right)\dfrac{\mathring{Q}_F}{\mathring{Q}}$

3. $\dfrac{dR}{dt} = \left(2fk_d I - k_i \dfrac{RM}{\mathring{Q}}\right)\dfrac{\mathring{Q}_F}{\mathring{Q}}$

4. $\dfrac{d\lambda_0}{dt} = \left(k_i \dfrac{RM}{\mathring{Q}} - k_t \dfrac{\lambda_0^2}{\mathring{Q}}\right)\dfrac{\mathring{Q}_F}{\mathring{Q}}$

5. $\dfrac{d\lambda_1}{dt} = \left(k_i \dfrac{RM}{\mathring{Q}} + k_p \dfrac{\lambda_0 M}{\mathring{Q}} - k_t \dfrac{\lambda_0\lambda_1}{\mathring{Q}}\right)\dfrac{\mathring{Q}_F}{\mathring{Q}}$

6. $\dfrac{d\lambda_2}{dt} = \left(k_i \dfrac{RM}{\mathring{Q}} + k_p M \dfrac{\lambda_0 + 2\lambda_1}{\mathring{Q}} - k_t \dfrac{\lambda_0\lambda_2}{\mathring{Q}}\right)\dfrac{\mathring{Q}_F}{\mathring{Q}}$

7. $\dfrac{d\mu_0}{dt} = \left(k_t \dfrac{\lambda_0^2}{\mathring{Q}}\right)\dfrac{\mathring{Q}_F}{\mathring{Q}}$

8. $\dfrac{d\mu_1}{dt} = \left(k_t \dfrac{\lambda_0\lambda_1}{\mathring{Q}}\right)\dfrac{\mathring{Q}_F}{\mathring{Q}}$

9. $\dfrac{d\mu_2}{dt} = \left(k_t \dfrac{\lambda_0\lambda_2}{\mathring{Q}}\right)\dfrac{\mathring{Q}_F}{\mathring{Q}}$

10. $\mathring{Q}_F = \dfrac{M_F(MW_m)}{\rho_{m,F}}$ (Assuming pure monomer)

11. $\mathring{Q} = \dfrac{M(MW_m)}{\rho_m} + \dfrac{(M_F - M)(MW_m)}{\rho_p}$

I.C.: at $t = 0$: $I = I_F$, $M = M_F$, $R = \lambda_k = \mu_k = 0$; ($k = 0, 1, 2$).

change with z. This would require the use of the much more complicated finite-element method for the integration of the partial differential equations, and computer codes like FLUENT, etc., would be required to integrate them. Because the units (and meanings) of I, M, R, λ_k, and μ_k ($k = 0, 1, 2$) are different in the two reactors, appropriate continuity equations must be written at the exit of the PFTR/entrance of the film reactor. These are given in Table III.

The equations describing the cage, gel (Trommsdorff) and glass effects are provided in Table IV, and the values of the several rate constants and the parameters[12] characterizing these three diffusion-controlled phenomena are given in Table V. Even though the density of the reaction mixture has been assumed constant (at the value corresponding to the feed to the film reactor) while developing the equations for the film reactor, changes in the density, ρ, are accounted for while estimating the rate constants in the presence of the cage, gel, and glass effects in this reactor. The equations for the three θs in Table IV use the local values of the concentrations, M/V_1 and λ_o/V_1, estimated using the local densities and concentrations of the monomer and polymer. By doing this, we obtain more accurate results for the section-average monomer conversions and molecular weights in the film reactor than if we had assumed the density to be constant in both Tables III and IV.

Expressions for the local monomer conversion, x_m, as well as the section-average value, $\bar{x}_m$, of the

Table III Model Equations for MMA Polymerization in the Film Reactor

0. $U_0 = \mathring{Q}_p/(2LW)$

1. $\dfrac{\partial I}{\partial z} = -k_d \dfrac{I}{U_0}$

2. $\dfrac{\partial M}{\partial z} = -k_p \dfrac{M\lambda_0}{U_0^2} - k_i \dfrac{RM}{U_0^2}$

3. $\dfrac{\partial R}{\partial z} = 2fk_d \dfrac{I}{U_0} - k_i \dfrac{RM}{U_0^2}$

4. $\dfrac{\partial \lambda_0}{\partial z} = k_i \dfrac{RM}{U_0^2} - k_t \dfrac{\lambda_0^2}{U_0^2}$

5. $\dfrac{\partial \lambda_1}{\partial z} = k_i \dfrac{RM}{U_0^2} + k_p \dfrac{M\lambda_0}{U_0^2} - k_t \dfrac{\lambda_0\lambda_1}{U_0^2}$

6. $\dfrac{\partial \lambda_2}{\partial z} = k_i \dfrac{RM}{U_0^2} + k_p M \dfrac{\lambda_0 + 2\lambda_1}{U_0^2} - k_t \dfrac{\lambda_0\lambda_2}{U_0^2}$

7. $\dfrac{\partial \mu_0}{\partial z} = k_t \dfrac{\lambda_0^2}{U_0^2}$

8. $\dfrac{\partial \mu_1}{\partial z} = k_t \dfrac{\lambda_0\lambda_1}{U_0^2}$

9. $\dfrac{\partial \mu_2}{\partial z} = k_t \dfrac{\lambda_0\lambda_2}{U_0^2}$

10. $\rho_{\text{mix}} U_0 C_{p,\text{mix}} \dfrac{\partial T}{\partial z} = (-\Delta H_r) k_p \dfrac{M\lambda_0}{U_0^2} + K_T \dfrac{\partial^2 T}{\partial y^2}$

I.C. $z = 0$, $I = I_{in} = I_p/(2LW)$; $M = M_{in} = M_p/(2LW)$; $R = R_{in} = R_p/(2LW)$; $\lambda_k = \lambda_{k,in} = \lambda_{k,p}/(2LW)$, $k = 0, 1, 2$; $\mu_k = \mu_{k,in} = \mu_{k,p}/(2LW)$, $k = 0, 1, 2$; $T = T_0$

B.C. $y = 0$: $T = T_w(z)$

y = L: $\partial T/\partial y = 0$

Table IV Cage, Gel, and Glass Effect Equations for Bulk Polymerizations[12]

$$\frac{1}{f} = \frac{1}{f_0}\left[1 + \theta_f(T)\frac{M}{V_1}\frac{1}{\exp[\xi_{13}\{-\psi + \psi_{\text{ref}}\}]}\right] \quad (1)$$

$$\frac{1}{k_t} = \frac{1}{k_{t,0}} + \theta_t(T)\mu_n^2\frac{\lambda_0}{V_1}\frac{1}{\exp[-\psi + \psi_{\text{ref}}]} \quad (2)$$

$$\frac{1}{k_p} = \frac{1}{k_{p,0}} + \theta_p(T)\frac{\lambda_0}{V_1}\frac{1}{\exp[\xi_{13}\{-\psi + \psi_{\text{ref}}\}]} \quad (3)$$

$$\psi = \frac{\gamma\left\{\dfrac{\rho_m\phi_m\hat{V}_m^*}{\xi_{13}} + \rho_p\phi_p\hat{V}_p^*\right\}}{\rho_m\phi_m\hat{V}_m^*V_{fm} + \rho_p\phi_p\hat{V}_p^*V_{fp}} \quad (4)$$

$$\psi_{\text{ref}} = \frac{\gamma}{V_{fp}} \quad (5)$$

$$V_1 = \frac{M(MW_m)}{\rho_m} + \frac{(\xi_{m1} - M)(MW_m)}{\rho_p} \quad (6)$$

$$\phi_m = \frac{M(MW_m)/\rho_m}{\dfrac{M(MW_m)}{\rho_m} + \dfrac{(\xi_{m1} - M)(MW_m)}{\rho_p}} \quad (7)$$

$$\xi_{m1} = M_F(\text{in PFTR}); \quad M_F/(2LW) \text{ in Film Reactor} \quad (8)$$

$$\phi_p = 1 - \phi_m \quad (9)$$

$$\xi_{13} = \frac{\hat{V}_m^*(MW_m)}{\hat{V}_p^*M_{jp}} \quad (10)$$

$$\xi_{13} = \frac{\hat{V}_I^*(MW_I)}{\hat{V}_p^*M_{jp}} \quad (11)$$

$$k_d = k_d^0\exp(-E_d/R_gT) \quad (12)$$

$$k_{p,0} = k_{p,0}^0\exp(-E_p/R_gT) \quad (13)$$

$$k_{t,0} = k_{t,0}^0\exp(-E_t/R_gT) \quad (14)$$

conversion in the film reactor at any axial location, z, can easily be written. The same is true for the section-average (cup-mixing) values of M_n and M_w at any axial location. The final expressions for these are given in Table VI.

The equations for the film reactor can be written in the following general form:

$$\partial\mathbf{x}/\partial z = \mathbf{f}(\mathbf{x}, \mathbf{u}) \quad (1a)$$

$$x_i(z = 0) = x_{i,p}/(2LW);\ i = 1, 2, \ldots, 9; \qquad x_{10}(z = 0) = T_o \quad (1b)$$

$$T(y = 0) = T_w(z) \quad (1c)$$

$$\partial T/\partial y(\text{at } y = L) = 0 \quad (1d)$$

where $\mathbf{x}$ is the vector of state variables, x_i, defined by

$$\mathbf{x} = [I, M, R, \lambda_0, \lambda_1, \lambda_2, \mu_0, \mu_1, \mu_2, T]^T \quad (2)$$

and $\mathbf{u}$ is the vector of decision variables, defined by:

Table V Parameters Used for Bulk Polymerization of MMA with AIBN[12]

ρ_m	$= 966.5 - 1.1(T - 273.15)$ kg/m^3
ρ_p	$= 1200$ kg/m^3
f_0	$= 0.58$
k_d^0	$= 1.053 \times 10^{15}$ s^{-1}
$k_{p,0}^0$	$= 4.917 \times 10^2$ m^3/mol−s
$k_{t,0}^0$	$= 9.8 \times 10^4$ m^3/mol−s
k_i	$= k_p$
E_d	$= 128.45$ kJ/mol
E_p	$= 18.22$ kJ/mol
E_t	$= 2.937$ kJ/mol
(MW_m)	$= 0.10013$ kg/mol
(MW_I)	$= 0.06800$ kg/mol
Parameters for the Cage, Gel, and Glass Effects	
$\hat{V}_I^*$	$= 9.13 \times 10^{-4}$ m^3/kg
$\hat{V}_m^*$	$= 8.22 \times 10^{-4}$ m^3/kg
$\hat{V}_p^*$	$= 7.70 \times 10^{-4}$ m^3/kg
M_{jp}	$= 0.18781$ kg/mol
γ	$= 1$
V_{fm}	$= 0.149 + 2.9 \times 10^{-4}[T(\text{K}) - 273.15]$
V_{fp}	$= 0.0194 + 1.3 \times 10^{-4}[T(\text{K}) - 273.15 - 105]$; for $T < (105 + 273.15)$ K
Correlations used for the θs	
$\log_{10}[\theta_t(T), s]$	$= a_1 - a_2\,(1/T) + a_3\,(1/T^2)$
$\log_{10}[\theta_p(T), s]$	$= b_1 - b_2\,(1/T) + b_3\,(1/T^2)$
$\log_{10}[10^3\theta_f(T),$ m^3 mol^{-1}]	$= c_1 - c_2\,(1/T) + c_3\,(1/T^2)$
a_1	$= 1.2408 \times 10^2$; $a_2 = 1.0314 \times 10^5$; $a_3 = 2.2735 \times 10^7$
b_1	$= 8.0593 \times 10^1$; $b_2 = 7.5000 \times 10^4$; $b_3 = 1.7650 \times 10^7$
c_1	$= 2.0160 \times 10^2$; $c_2 = 1.4550 \times 10^5$; $c_3 = 2.7000 \times 10^7$
Parameters for the Film Reactor[39–41]	
ρ_{mix}	$= 1{,}055.5$ kg/m^3
$C_{p,\text{mix}}$	$= 1.674$ kJ/kg-K
ΔH_r	$= -58.19$ kJ/mol
K_T	$= 0.13$ W/m-K

Table VI Definitions for the Film Reactor

Local Values

$$x_m = 1 - \frac{M(2LW)}{M_F}$$

$$M_n = MW_m \frac{(\lambda_1 + \mu_1)}{(\lambda_0 + \mu_0)}$$

$$M_w = MW_m \frac{(\lambda_2 + \mu_2)}{(\lambda_1 + \mu_1)}$$

Section-Average Values (at any z)

$$\bar{x}_m \equiv 1 - W \int_{y=0}^{y=2L} \frac{M}{M_F}\, dy$$

$$\bar{M}_n \equiv (MW_m) \frac{\displaystyle\int_{y=0}^{y=2L} (\lambda_1 + \mu_1)\, dy}{\displaystyle\int_{y=0}^{y=2L} (\lambda_0 + \mu_0)\, dy}$$

$$\bar{M}_w \equiv (MW_m) \frac{\displaystyle\int_{y=0}^{y=2L} (\lambda_2 + \mu_2)\, dy}{\displaystyle\int_{y=0}^{y=2L} (\lambda_1 + \mu_1)\, dy}$$

$$\overline{PDI} = \frac{\bar{M}_w}{\bar{M}_n}$$

$$\mathbf{u} = [T_0,\, I_F,\, x_{mp},\, L,\, b_1,\, b_2,\, b_3]^T \tag{3}$$

In the set of two reactors in this process, the first one is a PFTR, which is described by ordinary differential equations (ODEs) of the initial value kind (ODE-IVPs), given in Table II. These are integrated using the DIVPAG subroutine of the IMSL library for the given initial conditions, $[I_F, M_F, 0, 0, 0, 0, 0, 0, 0, T_o]^T$. The integration is stopped when the selected value of x_{mp} is attained. The DIVPAG subroutine uses Gear's technique for integrating a set of stiff ODEs[42] with a tolerance of 10^{-6}. The second reactor is the film reactor. This is described by partial differential equations (PDEs) of the boundary value kind (PDE-BVPs), given in Table III. The method of lines (finite differences) is used to convert these into a coupled set of several ODEs using the DSS002 code,[43] and DIVPAG is then used to solve them. It was assumed that the range, $0 \le y \le L$, had six equispaced grid points (increasing this number to 11, 21, or 31 gave similar final results). Instead of the method of lines, one could use the Orthogonal Collocation (OC) method[42] to convert the governing PDEs into sets of ODEs. However, for complex systems, as for example, for a nylon 6 tubular reactor, it has been demonstrated[44] that the OC method is not necessarily superior to the method of lines, and one cannot say a priori that OC would be better for a particular complex problem.

Two objective functions have been selected for the optimization of this process. The first is the maximization of the section-average value of the monomer conversion, $\bar{x}_{mf}$, at the end of the film reactor. Alternatively,[32] the value of $1/(1 + \bar{x}_{mf})$ could be minimized. The second objective function to be minimized is the length, z_f, of the film reactor. An end-point constraint is also used in our study, viz., the section-average value of the number-average molecular weight of the product polymer must attain a desired value, M_{nd}. It is to be noted that this requirement is imposed on the product at the exit of the film reactor only, and is not imposed globally, throughout the reactor. The end-point constraint is incorporated in our study by using it as a penalty function[21] with a weighting factor, w_1 ($= 10^4$), in the objective functions. The complete multiobjective optimization problem solved is, thus, written as follows:

$$\text{Min } \mathbf{I} \equiv [I_1,\, I_2]^T \tag{4a}$$

$$I_1 = \frac{1}{1 + \bar{x}_{mf}} + w_1 \left(1 - \frac{\bar{M}_{nf}}{M_{nd}}\right)^2 \tag{4b}$$

$$I_2 = z_f + w_1 \left(1 - \frac{\bar{M}_{nf}}{M_{nd}}\right)^2 \tag{4c}$$

Subject to (s.t.):

$$T_{\min} \le T \le T_{\max} \tag{5a}$$

$$\bar{M}_{nf} = M_{nd} \pm Tol \tag{5b}$$

$$\text{All equations (Tables 2 and 3)} \tag{5c}$$

The constraints in eq. (5) involve a global constraint on the temperature, T, at any location in the film. The lower limit is to ensure that the

temperature is reasonably high (this is difficult to ensure by the choice of bounds on the coefficients, b_1, b_2, and b_3, describing the wall temperature, T_w). The upper limit is to ensure that the local temperature inside the film does not become so high anywhere in the entire film as to cause degradation of the polymer. This constraint is implemented in the computer code by artificially assigning a very high value to the objective functions corresponding to the chromosomes where such a violation occurs ("killing" the chromosome instantaneously). In addition to using the end-point constraint on M_n as a penalty function [eqs. (4b) and (c)], we also impose an additional requirement on the section-average value of M_n. This represents an apparent redundancy, but is required because of the way our computer code for the integration of the ODEs works. Our code continues to integrate the ODEs until a very large value of z of 500 m before evaluating the objective functions, even if the end-point constraint on M_n is satisfied earlier. Hence, to avoid unnecessary waste of computational effort, we add a stopping condition (eq. (5b)), with a tolerance, *Tol*, of 0.1 kg/mol. Use of eq. (5b) thus saves computational time if the desired molecular weight is attained in a short length, while the penalty functions in eqs. (4b) and (4c) help in narrowing down the deviation from the desired value when the desired molecular weight cannot be attained even at z of 500 m. This is a numerical "trick" introduced to get rapid and good results. As long as the values of *Tol* and w_1 are selected appropriately, these two techniques of ensuring product of the right molecular weight are not contradictory.

The two objective functions used here are conflicting in nature and so it is likely that a Pareto set of nondominating optimal solutions is obtained. The nondominated sorting genetic algorithm (NSGA),[18,30] which is an adaptation of the simple genetic algorithm suited for multiobjective optimization problems, is used to solve the problem defined in eqs. (4) and (5). Details of this method are available in the literature,[18,30,33,38] but a short discussion together with a flowchart is given in Appendix 1.

It is mentioned in Table VII that the value of $\mathring{Q}_F$ is arbitrarily taken as 1 m^3/s, and that the cross-sectional areas, A_t and $2LW$, of the two reactors are (again, arbitrarily) taken as 1 m^2. These choices ensure that the velocities in both these reactors are of the order of 1 m/s. Because L and x_{mp} are decision variables, this implies that W and U_o are dependent variables in this study. We could, alternatively, have selected a fixed value of W, in which case U_o would have been a dependent variable. Yet again, W could have been selected as an additional decision variable. It is clear that several possibilities for formulating the optimization problem exist, but we illustrate the solution procedure only for the illustrative problem described in eqs. (4) and (5).

Table VII Parameters Used in this Study (Ref. Case)

NSGA Parameters
$N_{\text{gen}} = 40$
$N_p = 50$
$N_{ga} = 7$
$N_{str} = 32$
$p_c = 0.60$
$p_m = 0.00015$
$\sigma = 0.0496$
$\alpha_{sh} = 2$
Random seed = 0.6
Parameters for Optimization
$w_1 = 10^4$
$T_{\min} = 0$ °C
$T_{\max} = 150$ °C
$M_{nd} = 1.0 \times 10^3$ *kg/mol*
Tol = 0.1 kg/mol
Ranges of the Decision Variables
T_0: 50–60 °C
I_F: 20–25 mol/m^3
x_{mp}: 0.6–0.7
L: 0.001–0.01 m
b_1: −0.1–0.1 K/m
b_2: −0.01–0.01 K/m^2
b_3: −0.0001–0.0001 K/m^3
Reactor Parameters
$\mathring{Q}_F = 1$ m^3/s
$M_F = \rho_{mF} \mathring{Q}_F / MW_m$
$A_t = 1$ m^2
$2LW = 1$ m^2

RESULTS AND DISCUSSION

A computer code was written in FORTRAN 90 and tested for errors. The CPU time taken on an SGI Origin 2000 supercomputer for any typical optimization run (with 50 chromosomes over 40 generations, i.e., approximately 2000 simulations) was 315 s.

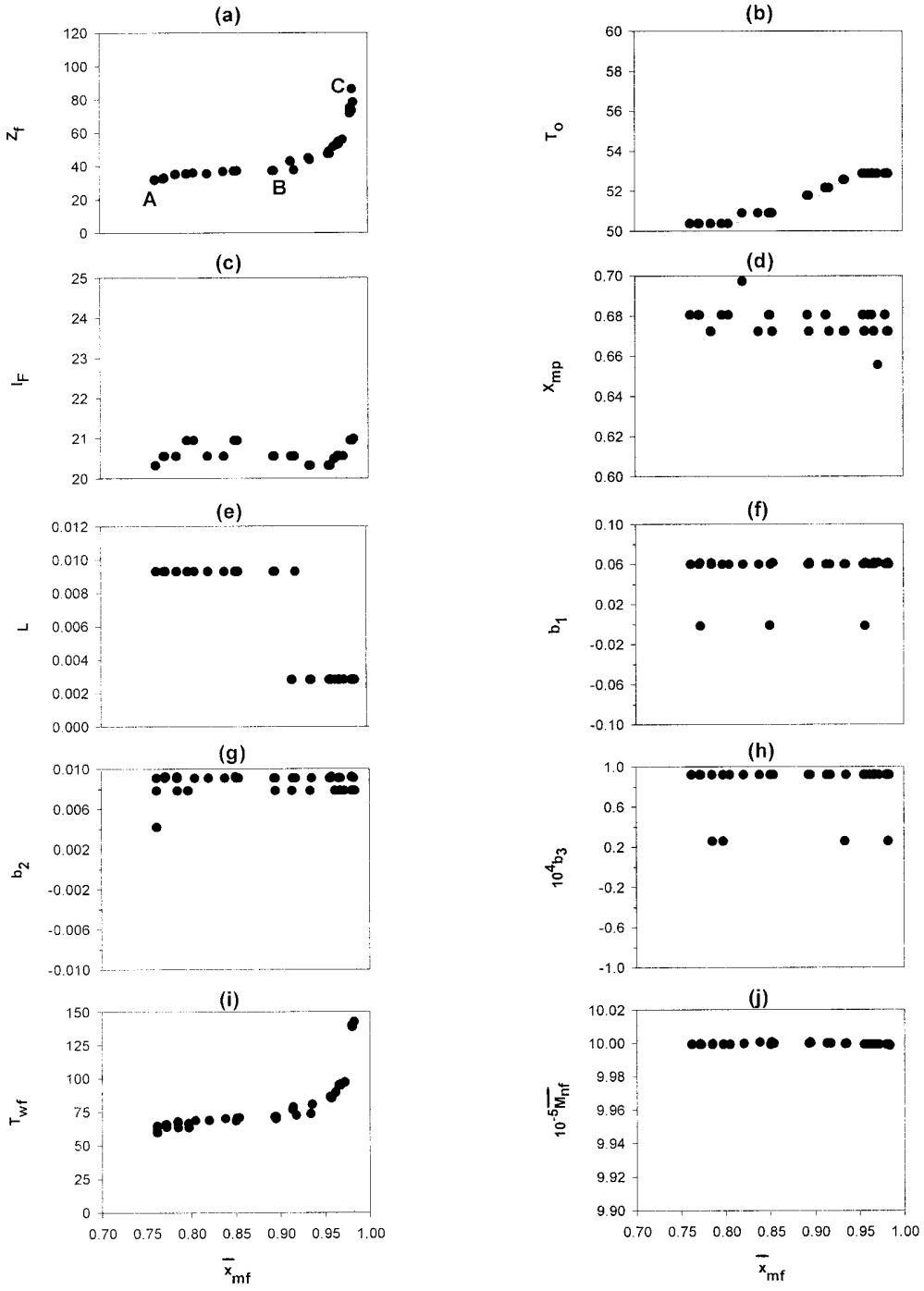

Figure 2 (a) Pareto set, (b–h) decision variables, (i) final wall temperature, T_{wf}, and (j) $\bar{M}_{\mathrm{nf}}$ at $N_g = 40$, under reference (Table VII) conditions. z_f and L in m; I_F in mol/s; T_o and T_{wf} in °C; $10^{-5}\ \bar{M}_{nf}$ in g/mol.

The parameters used in the first (reference) case are listed in Table VII. The ranges for the decision variables have been obtained after some trials with the program, so that meaningful results are obtained. Figure 2(a) shows the Pareto set under these conditions, at the end of 40 gen-

Table VIII Decision Variables for a Few Chromosomes of the Pareto Sets in Figure 3

Point	T_0 (°C)	I_F (mol/m^3)	x_{mp}	L (m)	b_1	b_2	b_3	$\bar{x}_{mf}$	z_f (m)	T_{wf} (°C)	$10^{-5}\,\bar{M}_{nf}$ (g/mol)	$\overline{PDI}_f$
A	50.37862	20.32137	0.68065	0.009285	0.059949	0.00908	0.000092	0.761865	31.8	64.43125	9.999272	12.06
B	52.15596	20.55347	0.67235	0.009285	0.059949	0.00908	0.000092	0.917441	37.75	72.32274	9.999768	10.50
C	52.87862	20.94637	0.68065	0.002817	0.059949	0.00783	0.000092	0.980064	74.91	140.0987	9.99906	10.60

erations ($N_g = 40$). Increasing N_g beyond 40 does not lead to any significant changes in these results. The two original objectives, $\bar{x}_{mf}$ and z_f, have been plotted in Figure 2(a), rather than I_1 and I_2 [given in eq. (4b) and (4c)]. It is clear that the points in Figure 2(a) indeed constitute a Pareto set, because, when we go from point B to point C, for example, one objective function (z_f) worsens while the other ($\bar{x}_{mf}$) improves. We have plotted the Pareto set up to fairly low values of $\bar{x}_{mf}$, even though the points at the higher end, above a mean conversion of about 0.9, would be more meaningful and useful. The Pareto set is observed to be quite flat at low values of $\bar{x}_{mf}$, but above mean conversions of about 0.95, it rises sharply. Figure 2(b)–(h) shows the seven decision variables corresponding to the different points on the Pareto set. Some amount of scatter is observed in these diagrams. Such scatter has also been observed in our earlier multiobjective optimization studies[34–37] of complex, large-scale industrial systems. The scatter could possibly be reduced somewhat (or even eliminated, by a suitable choice of computational parameters such as p_c, p_m, σ and α_{sh}) but at increased (and possibly unjustified) computational costs, as it requires a large number of trial runs to find appropriate values of these parameters. It is interesting to observe from these plots that in the more useful region of the Pareto set ($\bar{x}_{mf} > 0.9$), we would need to have lower values of the film thickness, higher temperatures in the PFTR, and higher initiator concentrations in the feed (to the PFTR). Also, the optimal values of x_{mp} are near its upper limit of 0.7. In fact, still higher values of x_{mp} would have been selected if we had chosen higher values for its upper bound, but these would not be too meaningful because it would be difficult to maintain isothermal conditions and ensure uniform velocity profiles in the PFTR at very high conversions.

Table VIII gives some details for the three points, A, B, and C, on the Pareto set of Figure 2(a). Figure 3 shows how the monomer conversion, M_n and PDI build up as a function of the axial location (z' in the PFTR, or $z'_p + z$ in the film reactor) in the two reactors for these three chromosomes. It should be noted that in Figure 3, the dotted lines represent the PFTR (values of the different variables as a function of z'), while the solid lines represent the film reactor (section-average values as a function of $z'_p + z$). Moreover, the inserts show enlarged views for the film reactor. It is observed that higher monomer conver-

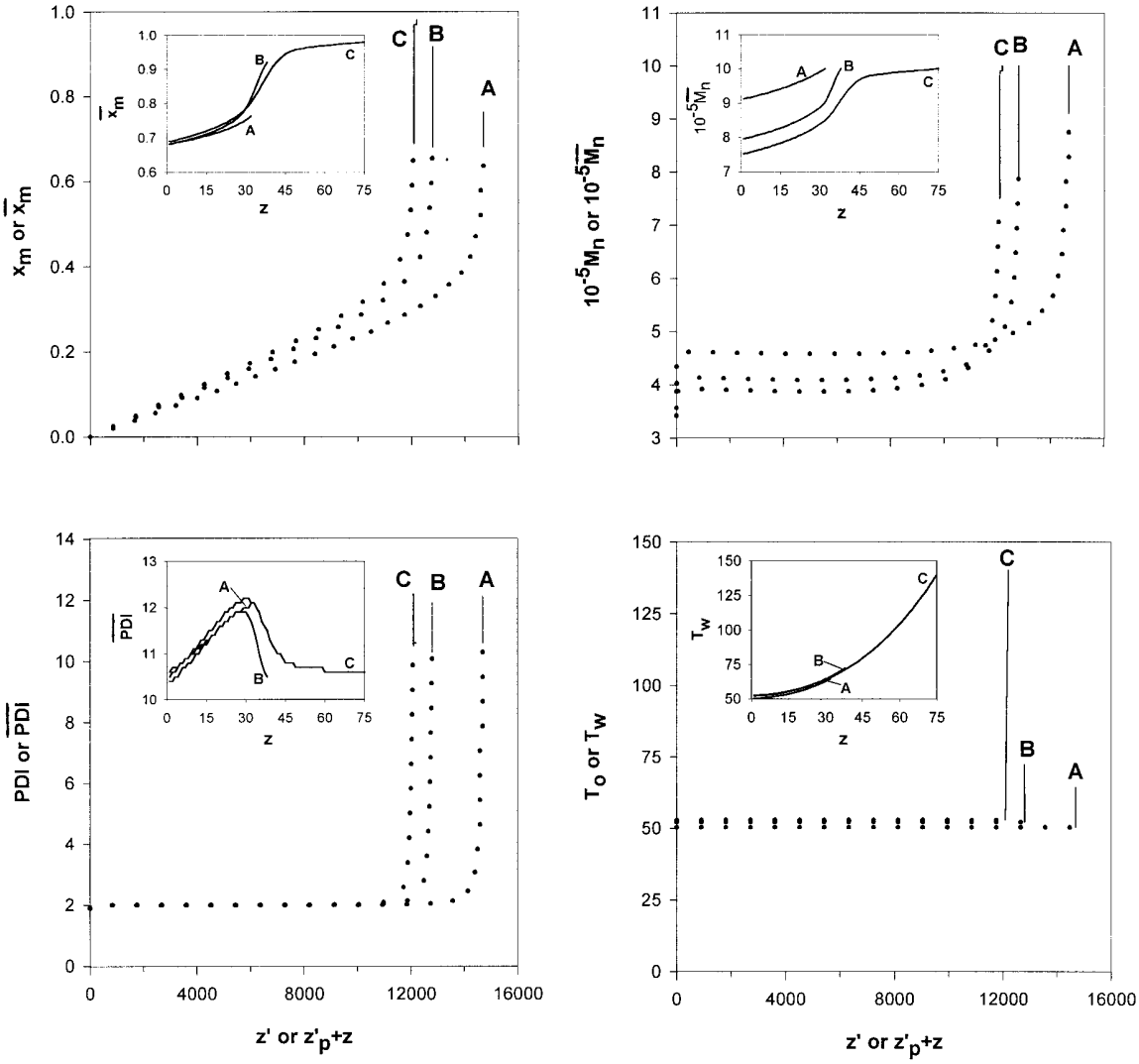

Figure 3 Monomer conversion, x_m, number-average molecular weight, M_n, polydispersity index, PDI, and temperature (T_o or T_w) as a function of the axial position (z' or $z'_p + z$) in the two reactors for chromosomes A, B, and C of Figure 2a. The dotted lines represent the PTFR (values as a function of z'), while the solid lines represent the film reactor (section-average values as a function of $z'_p + z$). $10^{-5}\,M_n$ g/mol; T_o and T_{wf} in °C. Inserts are the enlarged representations of the solid lines in the original figure (i.e., represents the film reactor only).

sions (and higher z_f, but lower $z'_p + z_f$) are attained for chromosome C by the use of higher I_F (which increases the rate of polymerization but lowers M_n), higher wall temperatures in the film reactor [see Fig. 2(i)] and thinner films (which hastens the gel effect to attain the desired molecular weight). The complex interplay of the several decision variables in influencing the optimal operation of the film casting operation can be observed. In fact, it is easier to explain the results once they are obtained—it would be nearly impossible to predict intuitively, optimal conditions in such complex cases. It is observed that the section-average values of the PDI of the polymer for cases B and C show maxima before the exit of the film reactor. Because the Pareto points between B and C represent the useful region, this means that incorporating PDI as another objective func-

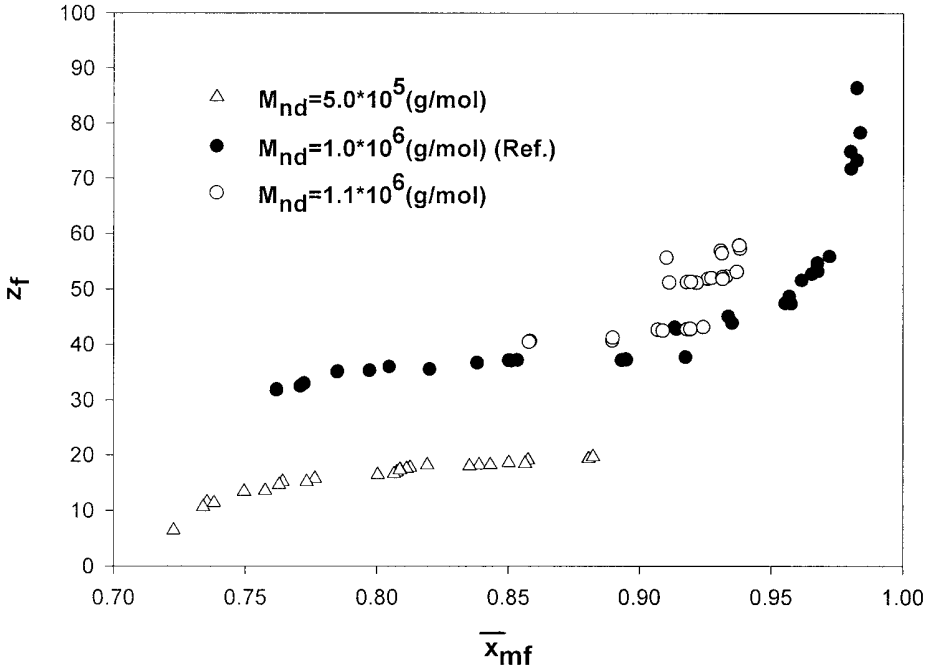

Figure 4 Pareto set for different values of M_{nd} (g/mol). The filled circles represent the reference case. z_f is in m.

tion in our study would not serve any useful purpose. Our present observation is also consistent with the earlier[33] inference for batch reactors that inclusion of the PDI as another objective function in the problem statement does not influence the optimal solutions. Figure 3 shows that

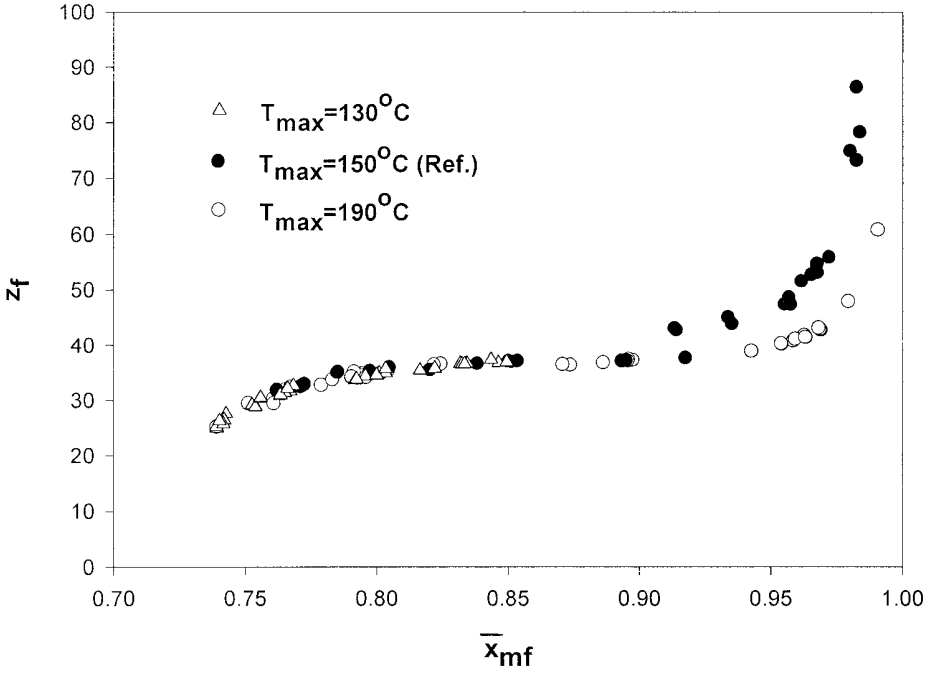

Figure 5 Pareto set for different values of $T_{\max}$ (°C). The filled circles represent the reference case. z_f is in m.

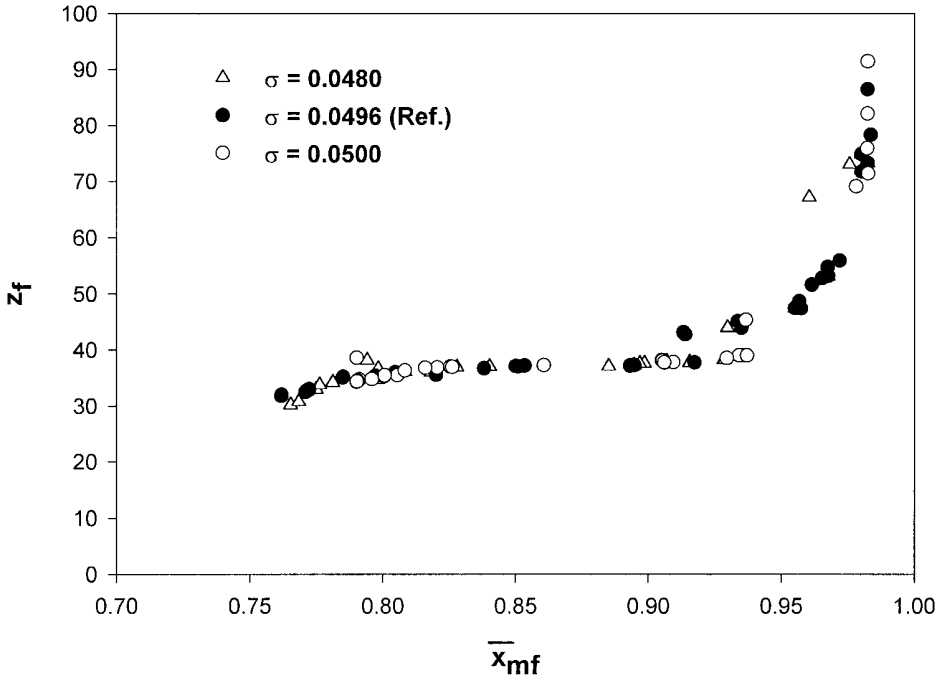

Figure 6 Influence of σ on the Pareto set. z_f is in m.

chromosome C requires higher wall temperatures in the film reactor to lead to high monomer conversions.

Satisfaction of the constraint on the final value of the section-average value of M_{nf} is illustrated in Figure 2(j). Figures 2(f)–(h) show that the co-

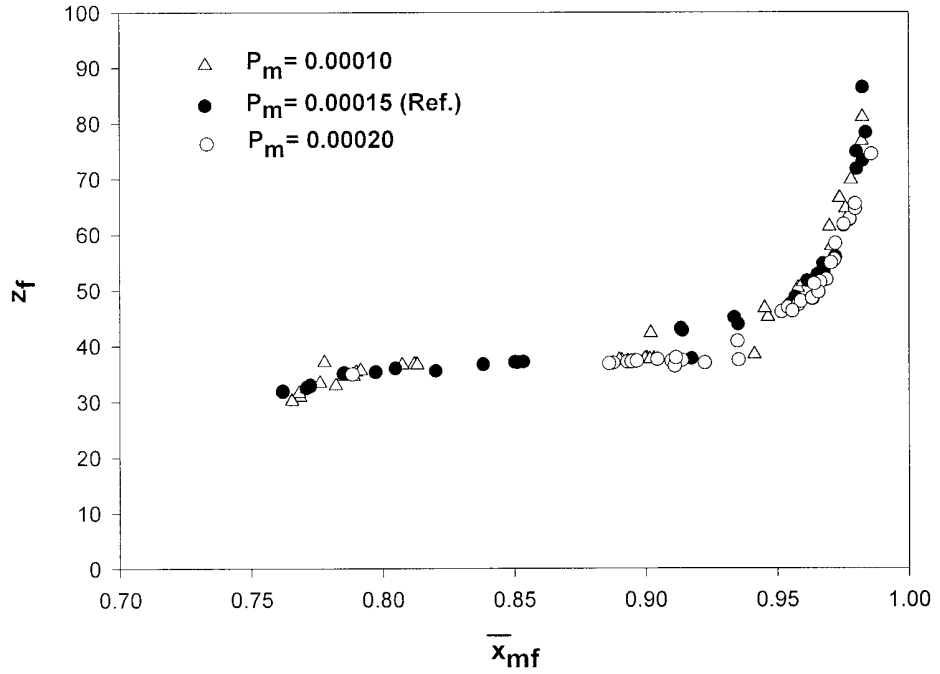

Figure 7 Influence of mutation probability on the Pareto set. z_f is in m.

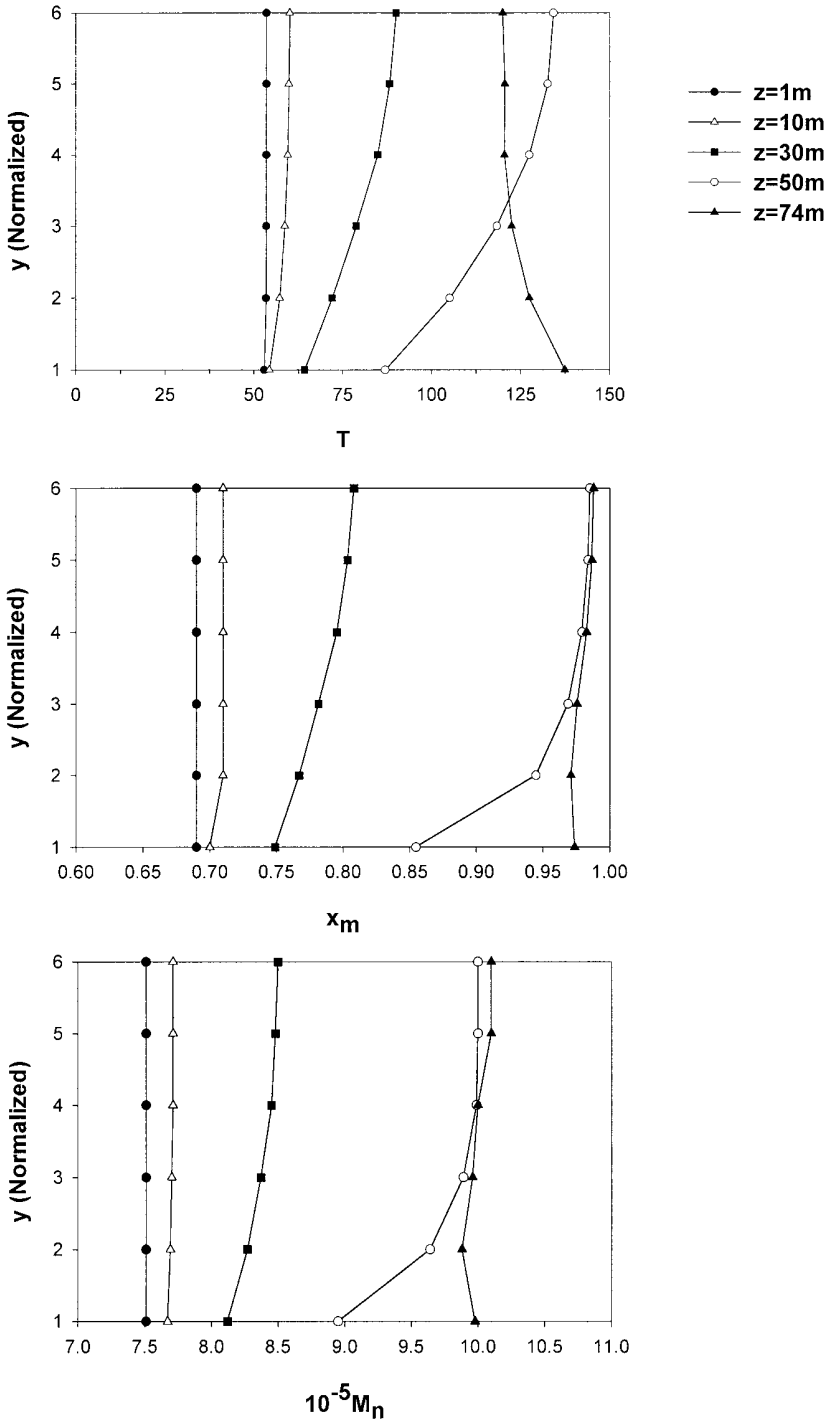

Figure 8 Variation of local values of T (°C), x_m and $10^{-5} M_n$ (g/mol) with y at different axial locations, z, for chromosome C in Figure 2a. y(normalized) = 1 + 5(y/L) = grid point number. y(normalized) = 1 corresponds to the wall.

efficients, b_1, b_2, and b_3, describing the wall temperature in the film reactor are positive under optimal conditions, even though negative values are permitted. This implies that the temperature at the wall increases monotonically with increasing z, in the film reactor. Figure 2(i) suggests that a second-order (quadratic) polynomial for the wall temperature profile could have been used as well. However, we used a higher order (cubic) polynomial because we did not know, *a priori*, what the optimal temperature profile would look like for this complex system, and we did not want to miss out the global optimum solution.

The affect of varying some of the parameters used (one at a time), on the Pareto set is now studied. Figure 4 shows the Pareto sets corresponding to different values of M_{nd}. When M_{nd} is lower than the reference value, the final value of $\bar{x}_{mf}$ is lower than what is possible for the reference case (all other parameters being unchanged). This is not surprising, because the reaction is stopped as soon as the end-point constraint on the average M_n is satisfied, even though there is plenty of unreacted monomer still left. For higher values of M_{nd}, also the reaction does not go to as high a value of the conversion, and there appears to be a maximum value of M_{nd} (at least for the set of parameters selected)! The higher values of M_{nd} are attained (diagram not shown) by the use of lower values of T_o and T_w.

Figure 5 shows the Pareto sets for different values of $T_{\max}$, the global constraint on the film temperature. This constraint is essential to ensure that degradation[40] of the polymer is avoided. It is observed that at higher values of $T_{\max}$, high conversions are attained at smaller values of z_f (by the use of slightly higher values of I_F and L; diagrams for these variables are not shown), which is expected. However, use of lower values of $T_{\max}$ prevents the attainment of high conversions (for the same M_{nd}). The attractiveness of using the highest possible value of $T_{\max}$ is to be noted.

The affect of reducing the weightage factor, w_1, to 10^3 (from the reference value of 10^4) is to increase the scatter of the points on the Pareto set. This is because use of lower w_1 makes the "penalty" term in eq. (4) too small, and therefore, suppresses the "death" of the bad chromosomes. Increase in w_1 to 10^5 does not influence the Pareto much.

It is well known[18] that the selection of the values of the several computational parameters in NSGA is quite important (see Appendix 1). Figures 6 and 7 show the results of varying σ and p_m, respectively. These diagrams show that the results obtained for different σ and p_m superpose, and that we could use different values of these parameters to obtain additional points on the Pareto set. The mutation probability, p_m, seems to be the most important. Varying the crossover probability, p_c, from 0.55 to 0.7 did not give very different results (and so these results are not shown). It should be mentioned that if a considerable number of trial runs were performed to determine suitable choices for the computational parameters (p_c, p_m, σ, and α_{sh}), it would have been possible to eliminate the scatter in the optimal solutions obtained (Figs. 2–5). However, this was not done because this would be computationally quite intensive, and the gains are minimal.

The variation of the local values of the temperature, monomer conversion, and M_n, with y and z, are shown in Figure 8 for the high-conversion chromosome C. Severe y-gradients are observed inside the film at values of z of about 30–50 m. The temperatures near the center of the film are found to be higher than at the wall, due to the exothermicity of the (fast) reaction until a z of about 50 m, as well as the low thermal conductivity of the polymer. This leads to higher values of both the monomer conversion and molecular weight near the center of the film. This also results in high values of the section-average PDI. As the reaction near the center gets completed and heat conduction takes over (for 50 m $\leq z \leq$ 74 m), this trend reverses. Higher values of T_w lead to higher temperatures near the wall. This enables the completion of the reaction (higher x_m) near the wall. The values of x_m and M_n are almost uniform across the film thickness by the time the reaction mass emerges from the reactor as the final product. This explains the decrease in the values of the section-average PDI (see Fig. 3) near the end of the film reactor.

CONCLUSIONS

A mathematical model for the continuous casting (cum polymerization) process of methyl methacrylate is developed. A multiobjective optimization (maximization of the average monomer conversion in the product and minimization of the length of the film reactor) of this process in the presence of constraints on molecular weight and temperature is then carried out. The robust

NSGA technique is used with seven decision variables. A Pareto set is obtained, which is comprised of a set of equally good (nondominating), optimal points. These provide an excellent starting point for a decision maker, who can then use his intuition and "gut feeling" to select one of these points for design or operation. The affect of varying the several parameters is also studied, to make the results more useful.

One of the authors (S.K.G.) wishes to acknowledge the hospitality and facilities provided by the Department of Chemical Engineering, University of Wisconsin, Madison, during the preparation of this manuscript.

NOMENCLATURE

A_t	cross-sectional area of the PFTR (m^2)
b_1, b_2, b_3	coefficients describing $T_w(z)$ (K/m, K/m^2, K/m^3)
$C_{p,\mathrm{mix}}$	specific heat of the reaction mixture in the film reactor (J/kg-K)
D_n	dead polymer molecule having n repeat units
E_d, E_p, E_t	activation energies for the reactions in Table V (kJ/mol)
f	initiator efficiency
f_o	initiator efficiency in the limiting case of zero diffusional resistance
$-\Delta H_r$	enthalpy of the propagation reaction (J/mol)
I	molar flow rate of initiator at any axial location in the PFTR (mol/s) or molar flow rate of initiator per unit transverse area at any axial location in the film reactor (mol/m^2-s)
$\mathbf{I}$	vector of objective functions
I_1, I_2	individual objective functions
k_d, k_i, k_p, k_t	rate constants for initiation, propagation and termination in the presence of the gel and glass effects (1/s, or m^3/mol-s)
$k_{i,0}$, $k_{p,0}$, $k_{t,0}$	intrinsic (in absence of cage, gel and glass effects) rate constants (m^3/mol-s)
k_d^0, $k_{p,0}^0$, $k_{t,0}^0$	frequency factors for intrinsic rate constants (1/s or m^3/mol-s)
K_T	thermal conductivity of the reaction mixture in the film reactor (W/m-K)
L	half the film thickness (m)
M	molar flow rate of monomer at any axial location in the PFTR (mol/s) or molar flow rate of monomer per unit transverse area at any axial location in the film reactor (mol/m^2-s)
M_{jp}	molecular weight of the polymer jumping unit (kg/mol)
M_n	number-average molecular weight [= (MW_m) $(\lambda_1 + \mu_1)/(\lambda_o + \mu_o)$] at any location in either of the two reactors (kg/mol)
M_w	weight-average molecular weight [= (MW_m) $(\lambda_2+\mu_2)/(\lambda_1+\mu_1)$] at any location in any of the two reactors (kg/mol)
(MW_I), (MW_m)	molecular weights of pure primary radicals, monomer (kg/mol)
N_g	generation number
N_{ga}	number of decision variables in $\mathbf{u}$
N_{gen}	maximum number of generations
N_p	total number of chromosomes in population
N_{str}	number of binary digits representing each of the decision variables
p_c	crossover probability
p_m	mutation probability
P_n	growing polymer radical having n repeat units
PDI	polydispersity index at any location of the film reactor
$\mathring{Q}$	volumetric flow rate at any location in the PFTR (m^3/s)
R	molar flow rate of primary radicals at any axial location in the PFTR (mol/s) or molar flow rate of primary radicals per unit transverse area at any axial location in the film reactor (mol/m^2-s)
R_g	universal gas constant (kJ/mol-K)
t	$A_t z'/\mathring{Q}_F$ in the PFTR (s)
T	temperature of the reaction mixture at any location (K)

T_o temperature of the isothermal PFTR (°C)
Tol allowed tolerance on M_{nd}
$\mathbf{u}$ vector of decision variables, u_1, u_2, . . .
U_o velocity (constant) of liquid in the film reactor (m/s)
V_1 volumetric flow rate (m^3/s) of reaction mixture at any axial location in the PFTR, or volumetric flow rate per unit transverse area at any axial location in the film reactor (m^3/m^2-s)
V_{fm},V_{fp} free volume of monomer and polymer
$\hat{V}_I^*$, $\hat{V}_m^*$, $\hat{V}_p^*$ specific critical hole free volumes of initiator, monomer, and polymer (m^3/kg)
w_1 weightage factor
W width of film (m)
$\mathbf{x}$ vector representing state variables
x_m monomer conversion at any location
y transverse position (from lower belt) in the film reactor (m)
z axial location in the film reactor (m)
z' axial location in the PFTR (m)

Greek Letters

α_{sh} exponent controlling the sharing effect in NSGA
γ overlap factor
σ maximum normalized distance in $\mathbf{u}$ space between any two chromosomes (solutions)
ξ_{ml} defined in Table IV
ξ_{13}, ξ_{I3} ratio of the molar volume of the monomer and initiator jumping unit to the critical molar volume of the polymer, respectively
θ_f, θ_p, θ_t parameters in the model for the cage, gel and glass effects, respectively (m^3/mol, s, s)
λ_k kth (k = 0, 1, 2, . . .) moment of live polymer radicals, P_n (mol/s in PFTR; mol/m^2-s in film reactor)
μ_k kth (k = 0, 1, 2, . . .) moment of dead polymer radicals, D_n (mol/s in PFTR; mol/m^2-s in film reactor)
μ_n number average chain length
ρ_m, ρ_p densities of pure (liquid) monomer and of pure polymer at any location (kg/m^3)
ρ_{mix} density (constant) of the reaction mixture in the film reactor (kg/m^3)
ϕ_m, ϕ_p volume fractions of monomer and polymer in the liquid at any location

Subscripts/Superscripts

d desired value
f final value (at $z = z_f$) at the end of the film reactor
F feed to the PFTR
in inlet of the film reactor
max maximum value
min minimum value
p product at the outlet of the PFTR
w value at the wall (y = 0 and $2L$) of the film reactor

Symbols

$\overline{\cdots}$ section-average at any axial location in the film reactor

APPENDIX 1: A NOTE ON GENETIC ALGORITHM[19–21]

GA is a search technique developed by Holland,[19] that mimics the process of natural selection and natural genetics. In this algorithm, a set of decision variables are first coded in the form of a set of randomly generated binary numbers (0 and 1), called strings or chromosomes, thereby creating a "population (gene pool)" of such binary strings. Each chromosome is then mapped into a set of real values of the decision variables, using the upper and lower bounds of each of these. A model of the process is then used to provide values of the objective function for each chromosome. The value of the objective function of any chromosome reflects its "fitness." The Darwinian principle of "survival of the fittest" is used to generate a new and improved gene pool (new generation). This is done by preparing a "mating pool," comprised of copies of chromosomes, the number of copies of any chromosome being proportional to its fitness (Darwin's principle). Pairs of chromosomes are then selected randomly, and pairs of daughter

chromosomes generated using operations similar to those in genetic reproduction. The gene pool evolves, with the fitness improving over the generations.

Three common operators are used in GA [called *s*imple GA (SGA), to distinguish it from its various adaptations] to obtain an improved (next) generation of chromosomes. These are referred to as reproduction, crossover, and mutation. Reproduction is the generation of the mating pool, where the chromosomes are copied probabilistically based on their fitness values. However, no new strings are formed in the reproduction phase. New strings are created using the crossover operator by exchanging information among pairs of strings in the mating pool. A pair of daughter chromosomes are produced by selecting a crossover site (chosen randomly) and exchanging the two parts of the pair of parent chromosomes (selected randomly from the mating pool). The effect of crossover may be detrimental or beneficial. It is hoped that the daughter strings are superior. If they are worse than the parent chromosomes, they will slowly die a natural death over the next few generations (the Darwinian principle at work). To preserve some of the good strings that are already present in the mating pool, not all strings in the pool are used in crossover. A crossover probability, p_c, is used, where only $100p_c$ percent of the strings in the mating pool are involved in crossover while the rest continue unchanged to the next generation. After a crossover is performed, mutation takes place. The mutation operator changes a binary number at any location in a chromosome from a 1 to a 0 and vice versa, with a small probability, p_m. Mutation is needed to create a point in the neighborhood of the current point, thereby achieving a local search around the current solution and to maintain diversity in the population. The entire process is repeated until some termination criterion is met (the specified maximum number of generations is attained, or the improvements in the values of the objective functions become lower than a specified tolerance).

The optimal solutions to a multiobjective function optimization problem are nondominated (or Pareto-optimal) solutions. To handle multiple objective functions and find Pareto-optimal solutions, the simple genetic algorithm (SGA) has been modified. The new algorithm, Nondominated Sorting Genetic Algorithm (NSGA), differs from SGA only in the way the selection operator works.

NSGA uses a ranking selection method to emphasize the good points and a niche method to create diversity in the population without losing a stable subpopulation of good points. In the new procedure, several groups of nondominated chromosomes from among all the members of the population at any generation are identified and classified into "fronts." Each of the members in a particular front is assigned a large, common, front fitness value (a dummy value) arbitrarily. To distribute the points in this (or any other) front evenly in the decision variable domain, the dummy fitness value is then modified according to a sharing procedure by dividing it by the niche count of the chromosome. The niche count is a quantity that represents the number of neighbors around it, with distant neighbors contributing less than those nearby. The niche count, thus, gives an idea of how crowded the chromosomes are in the decision variable space. Use of the shared fitness value for reproduction thus helps spread out the chromosomes in the front because crowded chromosomes are assigned lower fitness values. This procedure is repeated for all the members of the first front. Once this is done, these chromosomes are temporarily removed from consideration, and all the remaining ones are tested for nondominance. The nondominated chromosomes in this round are classified into the next front. These are all assigned a dummy fitness value that is a bit lower than the lowest shared fitness value of the previous front. Sharing is performed thereafter. The sorting and sharing is continued until all the chromosomes in the gene pool are assigned shared fitness values. The usual operations of reproduction, crossover, and mutation are now performed. It is clear that the nondominated members of the first front that have fewer neighbors will get the highest representation in the mating pool. Members of later fronts, which are dominated, will get lower representations (they are still assigned some low fitness values, rather than "killed," to maintain the diversity of the gene pool). Sharing forces the chromosomes to be spread out in the decision variable space. The population is found to converge very rapidly to the Pareto set. It is to be noted that any number of objectives (both minimization and maximization problems) can be solved using this procedure. A flowchart describing this technique is presented below.

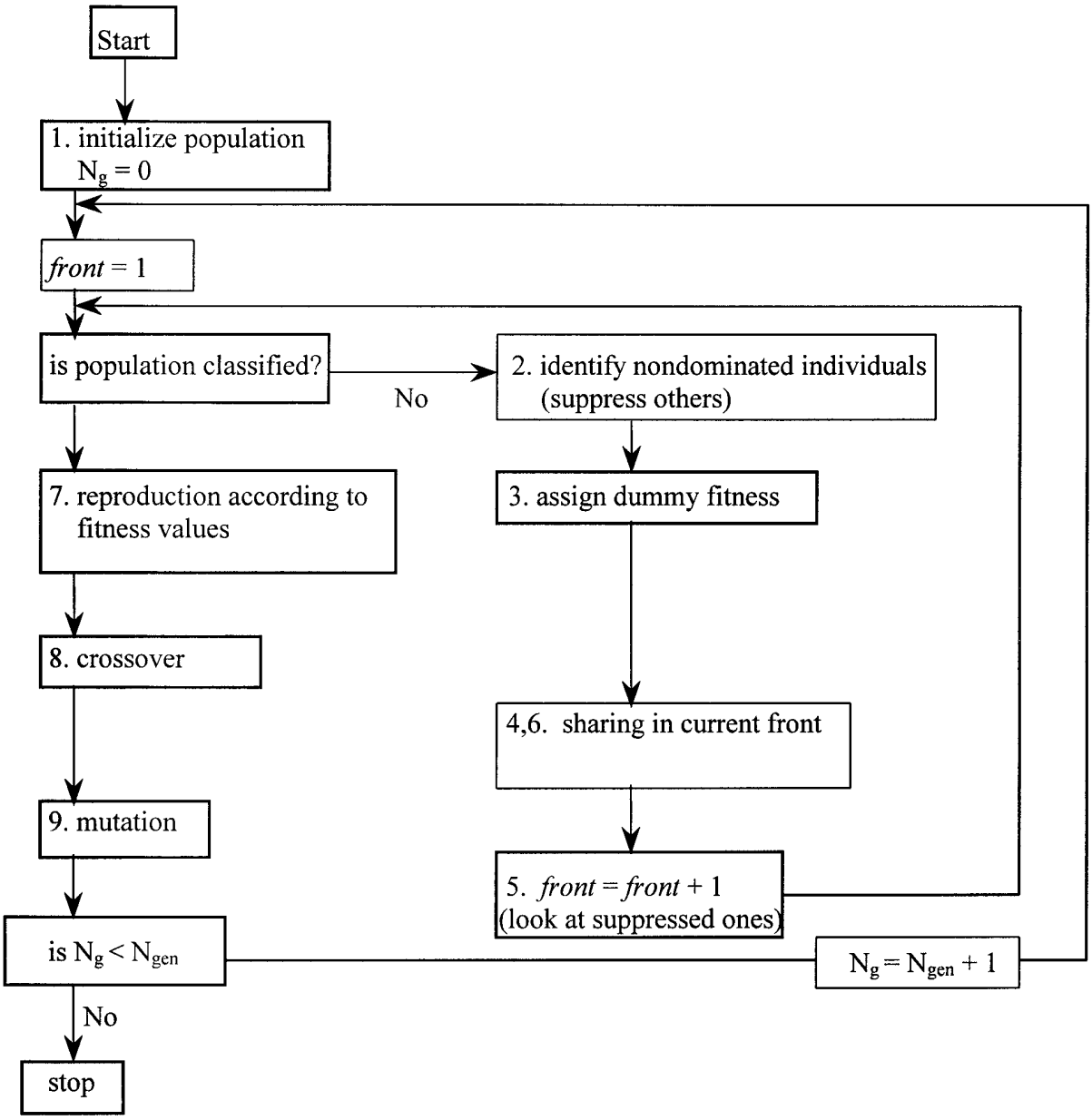

REFERENCES

1. Hui, A. W.; Hamielec, A. E. J Appl Polym Sci 1972, 16, 749.
2. Husain, A.; Hamielec, A. E. J Appl Polym Sci 1978, 22, 1207.
3. Soh, S. K.; Sundberg, D. C. J Polym Sci Polym Chem Ed 1982, 20, 1331.
4. Marten, F. L.; Hamielec, A. E. Am Chem Soc Symp Ser 1979, 104, 43.
5. Friis, N.; Hamielec, A. E. Am Chem Soc Div Polym Chem Polym Prepr 1975, 16, 192.
6. Ross, R. T.; Laurence, R. L. AIChE Symp Ser 1976, 72, 80.
7. Xie, T. Y.; Hamielec, A. E. Macromol Theory Simul 1993, 2, 455.
8. Chiu, W. Y.; Carratt, G. M.; Soong, D. S. Macromolecules 1983, 16, 348.
9. Achilias, D. S.; Kiparissides, C. J Appl Polym Sci 1988, 35, 1303.
10. Achilias, D. S.; Kiparissides, C. Macromolecules 1992, 25, 3739.
11. Ray, A. B.; Saraf, D. N.; Gupta, S. K. Polym Eng Sci 1995, 35, 1290.

12. Seth, V.; Gupta, S. K. J Polym Eng 1995, 15, 283.
13. Srinivas, T.; Sivakumar, S.; Gupta, S. K.; Saraf, D. N. Polym Eng Sci 1996, 36, 311.
14. Dua, V.; Saraf, D. N.; Gupta, S. K. J Appl Polym Sci 1996, 59, 749.
15. Gao, J.; Penlidis, A. J Macromol Sci Rev Macromol Chem Phys 1996, 36, 199.
16. Mankar, R. B.; Saraf, D. N.; Gupta, S. K. Ind Eng Chem Res 1998, 37, 2436.
17. Rodriguez, F. Principles of Polymer Systems; Taylor & Francis: Washington DC, 1996, 4th ed.
18. Srinivas, N.; Deb, K. Evol Comput 1995, 2, 3.
19. Holland, J. H. Adaptation in Natural and Artificial Systems; University of Michigan Press: Ann Arbor, MI, 1975.
20. Goldberg, D. E. Genetic Algorithms in Search, Optimization and Machine Learning; Addison-Wesley: Reading, MA, 1989.
21. Deb, K. Optimization for Engineering Design: Algorithms and Examples; Prentice Hall of India: New Delhi, 1996.
22. Farber, J. N. In Handbook of Polymer Science and Technology; Cheremisinoff, N. P., Ed.; Marcel Dekker: New York, 1989, p. 429, vol. 1.
23. Tieu, D.; Cluett, W. R.; Penlidis, A. Polym React Eng 1994, 2, 275.
24. Ray, W. H. Advanced Process Control; Butterworths: New York, 1989.
25. Bryson, A. E.; Ho, Y.C. Applied Optimal Control; Blaisdell: Waltham, MA, 1969.
26. Lapidus, L.; Luus, R. Optimal Control of Engineering Process; Blaisdell: Waltham, MA, 1967.
27. Vaid, N. R.; Gupta, S. K. Polym Eng Sci 1991, 31, 1708.
28. Ray, A. K.; Gupta, S. K. J Appl Polym Sci 1985, 30, 4529.
29. Ray, A. K.; Gupta, S. K. Polym Eng Sci 1986, 26, 1033.
30. Mitra, K.; Deb, K.; Gupta, S. K. J Appl Polym Sci 1998, 69, 69.
31. Chankong, V.; Haimes, Y. Y. Multiobjective Decision Making—Theory and Methodology; Elsevier, New York, 1983.
32. Chakravarthy, S. S. S.; Saraf, D. N.; Gupta, S. K. J Appl Polym Sci 1997, 63, 529.
33. Garg, S.; Gupta, S. K. Macromol Theory Simul 1999, 8, 46.
34. Bhaskar, V.; Gupta, S. K.; Ray, A. K. AIChE J 2000, 46(5), 1046.
35. Rajesh, J. K.; Gupta, S. K.; Rangaiah, G. P.; Ray, A. K. Ind Eng Chem Res 2000, 39, 706.
36. Yuen, C. C.; Aatmeeyata; Gupta, S. K.; Ray, A. K. J Membr Sci 2000, 176(2), 177.
37. Ravi, G.; Gupta, S. K.; Ray, M. B. Ind Eng Chem Res, in press.
38. Bhaskar, V.; Gupta, S. K.; Ray, A. K. Rev Chem Eng 2000, 16(1), 1.
39. Vargaftik, N. B. Handbook of Thermal Conductivity of Liquids and Gases; CRC Press: Boca Raton, FL, 1994.
40. Mark, H. F.; Bikales, N. M.; Overberger, C. G.; Menges, G. Encyclopedia of Polymer Science and Engineering; Wiley: New York, 1986, 2nd ed., vol 4.
41. Louie, B. M.; Soong, D. S. J Appl Polym Sci 1985, 30, 3707.
42. Gupta, S. K. Numerical Methods for Engineers; New Age International: New Delhi, 1995.
43. Schiesser, W. E. The Numerical Method of Lines; Academic: New York, 1991.
44. Jana, A. K.; Gupta, S. K. J Polym Eng 1990, 9, 23.